ANTIMICROBIAL AGENTS AND CHEMOTHERAPY, Aug. 2010, p. 3132–3142 Vol. 54, No. 8
0066-4804/10/$12.00 doi:10.1128/AAC.00124-10

Damage of the Bacterial Cell Envelope by Antimicrobial Peptides Gramicidin S and PGLa as Revealed by Transmission and Scanning Electron Microscopy▽

Mareike Hartmann,[1] Marina Berditsch,[1] Jacques Hawecker,[2] Mohammad Fotouhi Ardakani,[2] Dagmar Gerthsen,[2] and Anne S. Ulrich[1,3]*

Karlsruhe Institute of Technology (KIT), DFG Center for Functional Nanostructures (CFN), Institute of Organic Chemistry, Fritz-Haber-Weg 6, 76131 Karlsruhe, Germany[1]; Karlsruhe Institute of Technology (KIT), Laboratory for Electron Microscopy, DFG Center for Functional Nanostructures (CFN), Engesserstraße 7, 76131 Karlsruhe, Germany[2]; and Karlsruhe Institute of Technology (KIT), Institute of Biological Interfaces (IBG-2), P.O. Box 3640, 76021 Karlsruhe, Germany[3]

Received 28 January 2010/Returned for modification 9 April 2010/Accepted 28 May 2010

Scanning electron microscopy (SEM) and transmission electron microscopy (TEM) were used to examine the ultrastructural changes in bacteria induced by antimicrobial peptides (AMPs). Both the β-stranded gramicidin S and the α-helical peptidyl-glycylleucine-carboxyamide (PGLa) are cationic amphiphilic AMPs known to interact with bacterial membranes. One representative Gram-negative strain, *Escherichia coli* ATCC 25922, and one representative Gram-positive strain, *Staphylococcus aureus* ATCC 25923, were exposed to the AMPs at sub-MICs and supra-MICs in salt-free medium. SEM revealed a shortening and swelling of the *E. coli* cells, and multiple blisters and bubbles formed on their surface. The *S. aureus* cells seemed to burst upon AMP exposure, showing open holes and deep craters in their envelope. TEM revealed the formation of intracellular membranous structures in both strains, which is attributed to a lateral expansion of the lipid membrane upon peptide insertion. Also, some morphological alterations in the DNA region were detected for *S. aureus*. After *E. coli* was incubated with AMPs in medium with low ionic strength, the cells appeared highly turgid compared to untreated controls. This observation suggests that the AMPs enhance osmosis through the inner membrane, before they eventually cause excessive leakage of the cellular contents. The adverse effect on the osmoregulatory capacity of the bacteria is attributed to the membrane-permeabilizing action of the amphiphilic peptides, even at low (sub-MIC) AMP concentrations. Altogether, the results demonstrate that both TEM and SEM, as well as appropriate sample preparation protocols, are needed to obtain detailed mechanistic insights into peptide function.

Antimicrobial peptides (AMPs) are produced by most living organisms as a part of their innate immune system against bacteria, viruses, and fungi. They tend to be shorter than 45 amino acids, cationic, and amphipathic (20). These features define their ability to interact with the negatively charged lipids of bacterial membranes, leading to a destabilization and permeabilization of the cell membrane (50), multiple stresses on membrane proteins (42), and leakage of the cell content (30, 35). Due to the increasing resistance of pathogenic bacteria to conventional antibiotics and drugs, AMPs are a promising alternative for treating infections. Despite extensive research over the last decade, the exact mode of action of AMPs is not yet fully understood. Several models for the interaction of α-helical AMPs with the membranes, such as "barrel stave," "toroidal pore," or "carpet model," were postulated (46). All of these modes of action have in common that in the end the bacterial membrane is severely damaged, which can lead to the death of the cells. Over the last several years, increasing consideration was also given to the impact of AMPs on the function of membrane-associated enzyme systems (42, 55).

The (inner) bacterial cell membrane is responsible for many essential functions: transport, osmoregulation and respiration processes, biosynthesis and cross-linking of peptidoglycan, and synthesis of lipids. It is doubtless that for all these functions membrane integrity is absolutely necessary, and its disturbance can directly or indirectly cause metabolic dysfunction and cell death, besides pore formation *per se* (42). Observing alterations in bacterial membrane integrity by electron microscopy (EM) can help to clarify the detailed mechanisms of cell death at lethal AMP concentrations, but until now only a few AMPs have been investigated ultrastructurally. For example, permeabilization of the outer and inner membranes of Gram-negative bacteria has been described after exposure to defensins, as indicated by the leakage of electron-dense material (29). EM studies of the Gram-positive bacterium *Staphylococcus aureus* 209P treated with defensins showed mesosome-like structures and detached cell walls, but only protoplasts were lysed completely even with small amounts of peptide (47). This observation suggested that defensins have a stronger impact on the cytoplasmic membrane than on the cell wall. On the other hand, incubation of *S. aureus* ATCC 25923 and NCTC 4163 with other cationic AMPs resulted in thinning (14) or disintegration of the cell wall and in total cell lysis (5), respectively, which also points to a destabilization of the peptidoglycan layer by AMPs. The effects of peptidyl-glycylleucine-carboxyamide

* Corresponding author. Mailing address: KIT, IOC, Fritz-Haber-Weg 6, 76131 Karlsruhe, Germany. Phone and fax: 49-0721-6083912. E-mail: anne.ulrich@kit.edu.

▽ Published ahead of print on 7 June 2010.

(PGLa), magainin 2, melittin, and Sushi peptides on cell envelopes have been imaged by atomic force microscopy (AFM) of living Gram-negative bacteria in culture medium (12, 30, 35). It was shown that all peptides are lytic toward *Escherichia coli* and that especially the polar regions of the cells were susceptible. Clear alterations of the cell surface structure, e.g., change from smooth to rough, decreased surface stiffness, formation of micelles, and total cell rupture, were observed.

Here, we have chosen two representative antimicrobial peptides which have a slight bias for either Gram-positive or Gram-negative bacteria and which display distinctly different structures. Gramicidin S (GS) and PGLa are characterized by a β-stranded and an α-helical conformation, respectively, and their behavior in model lipid membranes has been thoroughly investigated by our group using solid-state nuclear magnetic resonance (NMR) (1–3, 17). To extend the current, quasiatomistic picture of these AMPs in terms of their morphological impact on the native membranes of living bacteria, we have now used EM to examine the bacterial morphology after treatment with GS and PGLa.

GS is a cyclic decapeptide [cyclo-(d-FPVOL)$_2$], produced by the rough phenotypes of the soil bacterium *Aneurinibacillus migulanus* (formerly *Bacillus brevis*) (16). It is particularly active against Gram-positive bacteria and, to a lesser extent, also against Gram-negative ones (23), *Mycoplasma* species (41), fungi (26), and viruses (9). The MIC against different *E. coli* strains lies between 3 and 12.5 μg/ml, and that against *S. aureus* lies at 1.5 μg/ml (26). Since GS shows hemolytic activity at 12 to 40 μg/ml (23, 27), its intravenous use is restricted, but local application is successful for the treatment of acute subcutaneous inflammation, infected wounds, and burns (15). The symmetric cyclic β-stranded backbone is amphiphilic due to two basic ornithine side chains on one face and hydrophobic residues on the other (31). Even though the exact mode of action of GS is still not clear, NMR studies have shown that the peptide binds flat onto the cytoplasmic membrane at a low concentration, and it can realign and assemble into a vertically inserted oligomer at a higher peptide concentration (1). The formation of discrete transmembrane pores has been postulated via membrane bending (22), via an assembly of β-barrels from stacked GS hexamers (18), or via double-stranded helical channels (31).

PGLa is an α-helical peptide of 21 amino acids (GMASKA GAIAGKIAKVALKAL-NH_2) from the magainin family produced by the African clawed frog *Xenopus laevis*. It has an amphipathic structure due to four basic lysine residues on one helical face (6), and it can destroy bacteria by interacting with their lipid membrane (11, 13). PGLa can kill bacteria, viruses, and fungi (10, 49), and it shows a low 50% hemolytic activity (HC_{50}) of 165 μg/ml (45). The MIC against various *E. coli* strains lies between 10 and 50 μg/ml, and that against *S. aureus* lies between 50 and 100 μg/ml (49). NMR studies with oriented model membranes have shown that at low concentrations the PGLa helices are bound to the membrane surface but that at higher concentrations they dimerize and can tilt into the membrane, where they assemble into a transmembrane oligomeric structure such as a toroidal pore (3).

In the present study, electron microscopy not only could reveal the direct damage on the bacterial envelope caused by GS and PGLa, but it also demonstrated a breakdown of the osmoregulatory capacity of *E. coli* and showed an effect on the intracellular DNA region in *S. aureus*.

MATERIALS AND METHODS

Peptides. GS was extracted from the producer cells of *A. migulanus* DSM 5759 as described previously (7). PGLa was synthesized at our PepSy labs (KIT, Karlsruhe, Germany). Both peptides were purified by reversed-phase high-pressure liquid chromatography (HPLC). A highly concentrated stock solution of GS was prepared in 50% ethanol, and a solution of PGLa was prepared in sterile demineralized water that had been purified with a Milli-Q Biocel system (Millipore, Bedford, MA).

Bacteria. Both strains, *E. coli* DSM 1103 (=ATCC 25922) and *S. aureus* DSM 1104 (=ATCC 25923), belong to the bacteria used for studying antibacterial activity according to the German Standard (DIN 58940). They were received from the Deutsche Sammlung von Mikroorganismen und Zellkulturen (DSMZ, Braunschweig, Germany).

Determination of MIC. MIC tests were performed by a standard broth microdilution assay (4) in microtiter plates from Nunc GmbH & Co. KG (Wiesbaden, Germany) to find out which sub- and supra-MICs should be used to treat the bacteria for the EM sample preparation. Since a high cell density of about 10^8 to 10^{10} CFU/ml is needed to observe EM images, the MIC for each peptide was also determined with high inoculation doses, 10^{10} CFU/ml for *E. coli* and 10^8 CFU/ml for *S. aureus*, in parallel with the usually used inoculum dose of 10^5 CFU/ml. Serial dilutions of the peptides were made in salt-free Luria broth (LB) medium, containing 10 g/liter tryptone and 5 g/liter yeast extract, but no salts, as recommended earlier by Kondejewski et al. (28). Test cultures, inoculated with cells grown overnight, were obtained in standard LB medium with 10 g/liter sodium chloride by cultivation up to mid-exponential growth phase (*E. coli* optical density at 550 nm [OD_{550}], ~4.0; *S. aureus* OD_{550}, ~5.5). The cells were then resuspended in salt-free LB medium for inoculation of microtiter plates. The wells of the microtiter plates, filled with 50 μl of graded peptide dilutions in salt-free LB medium, were then inoculated with 50 μl of the test organism up to the desired inoculation density. After incubation at 37°C for 20 h, the MIC was taken as the lowest concentration at which no growth was observed.

Preparation of cells for SEM. Bacteria of the mid-exponential growth phase were diluted with salt-free LB medium to the cell density mentioned above and treated accordingly with sub- and supra-MICs of GS or PGLa (see Table 1) for 1 h at 37°C. Untreated controls were prepared both in standard and in salt-free LB medium. For samples on silicon supports (Plano, Wetzlar, Germany), the bacteria were fixed with 2% glutaraldehyde, washed and resuspended in water, and then deposited onto silicon platelets as a 1-μl droplet. For samples on membrane filters, 10 μl of the treated cell suspension was placed onto a 0.45-μm-pore-size membrane filter (Schleicher & Schuell, Dassel, Germany), fixed for 1 h with 2% glutaraldehyde, washed, and postfixed with 1% (*E. coli*) or 0.2% (*S. aureus*) OsO_4. The samples were dehydrated with graded ethanol series, including *en bloc* staining with 3% uranyl acetate in 30% ethanol, and then air dried. For washing and dilution of fixing reagents, 0.15 M sodium phosphate buffer (pH 7.2) was used. All reagents used were EM grade and purchased from Polysciences (Eppelheim, Germany). A small amount of platinum was sputtered on the samples to avoid charging in the microscope. Microscopy was performed with a Zeiss Supra 55VP (Oberkochen, Germany) microscope. Secondary electron images were taken at low electron energies between 2 keV and 2.5 keV.

Preparation of cells for TEM. Bacteria for TEM samples were grown and incubated with AMPs as described above for SEM sample preparation. Controls were prepared also in standard and in salt-free LB medium. Cell pellets were obtained from 10 ml of each control or treated cell suspension and fixed with glutaraldehyde and OsO_4 as described above. The same buffers and dehydration protocol were used, followed, however, by graded acetone series and embedding in epoxy resin (Embed-It low-viscosity epoxy kit; Polysciences). Ultrathin sections were prepared on Formvar-coated grids (Plano, Wetzlar, Germany) and stained with 3% uranyl acetate. Microscopy was performed with a Zeiss 912 Omega (Oberkochen, Germany) microscope at 120-keV electron energy. To optimize the contrast, zero-loss energy filtering (43) was applied.

RESULTS

MIC values at different initial cell densities. The cell density has to be sufficiently high for high-magnification EM imaging. To identify the appropriate sub- and supra-MICs for these experiments, it was necessary to compare the MIC at standard

TABLE 1. MICs at different initial cell densities and peptide concentrations used for TEM and SEM sample preparation

MIC	Concn (μg/ml)[a]			
	E. coli		*S. aureus*	
	GS	PGLa	GS	PGLa
MIC under standard cell density[b]	8	16	1	8
MIC at high cell density suitable for EM[c]	16	32	8	32
Sub-MIC for TEM	8	20	4	20
Supra-MIC for TEM	40	100	20	100
Sub-MIC for SEM on silicon platelets	8	20	4	20
Supra-MIC for SEM on silicon platelets	40	100	20	100
Sub-MIC for SEM on membrane filter	8	10	4	10
Supra-MIC for SEM on membrane filter	40	50	20	50

[a] GS, gramicidin S; PGLa, peptidyl-glycylleucine-carboxyamide.
[b] For *E. coli*, OD_{670} was 0.001, and for *S. aureus*, OD_{670} was 0.002.
[c] For *E. coli*, OD_{670} was 0.1, and for *S. aureus*, OD_{670} was 0.3.

inoculation cell density with an approximately 100-fold-higher concentration. The results of these determinations are given in Table 1, showing that MIC values were increased 2-fold for *E. coli* and 4- to 8-fold for *S. aureus*. The corresponding sub- and supra-MICs for incubating the bacteria with GS and PGLa are presented in Table 1. Since *S. aureus* is more susceptible to GS, we had to treat *S. aureus* with concentrations of GS 2-fold lower than those for *E. coli*. The activities of PGLa against the strains are more similar, so we used the same concentrations to treat the two strains for TEM and SEM on silicon platelets and a 2-fold-lower concentration for SEM on membrane filters.

Scanning electron microscopy. The untreated *E. coli* cells, prepared for SEM micrographs in standard LB medium, were about 3.5 μm long and displayed a smooth and intact surface (Fig. 1A and 2A). The surface of the cells in medium with low ionic strength looked corrugated, and there were some dimples in these cells, but their average length remained unaltered (Fig. 1B and 2B). After incubation with sub- or supra-MICs of

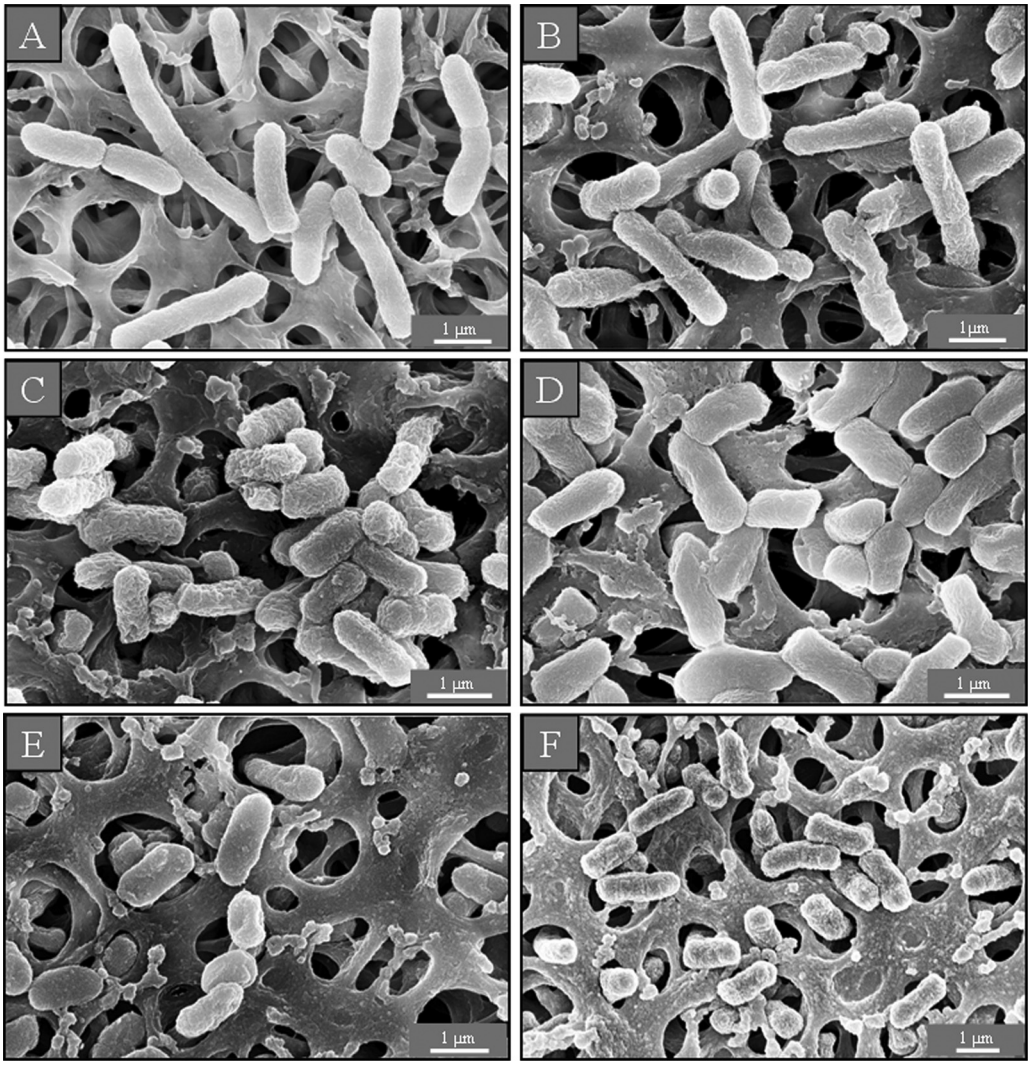

FIG. 1. SEM micrographs of untreated *E. coli* on membrane filters. In isotonic medium the cells are long and intact (A), whereas under low-salt conditions the surface of the bacteria looks corrugated (B). After AMP treatment with a sub-MIC (C) (8 μg/ml) or a supra-MIC (D) (40 μg/ml) of GS and with a sub-MIC (E) (10 μg/ml) or a supra-MIC (F) (50 μg/ml) of PGLa, the cells look shorter and more compact.

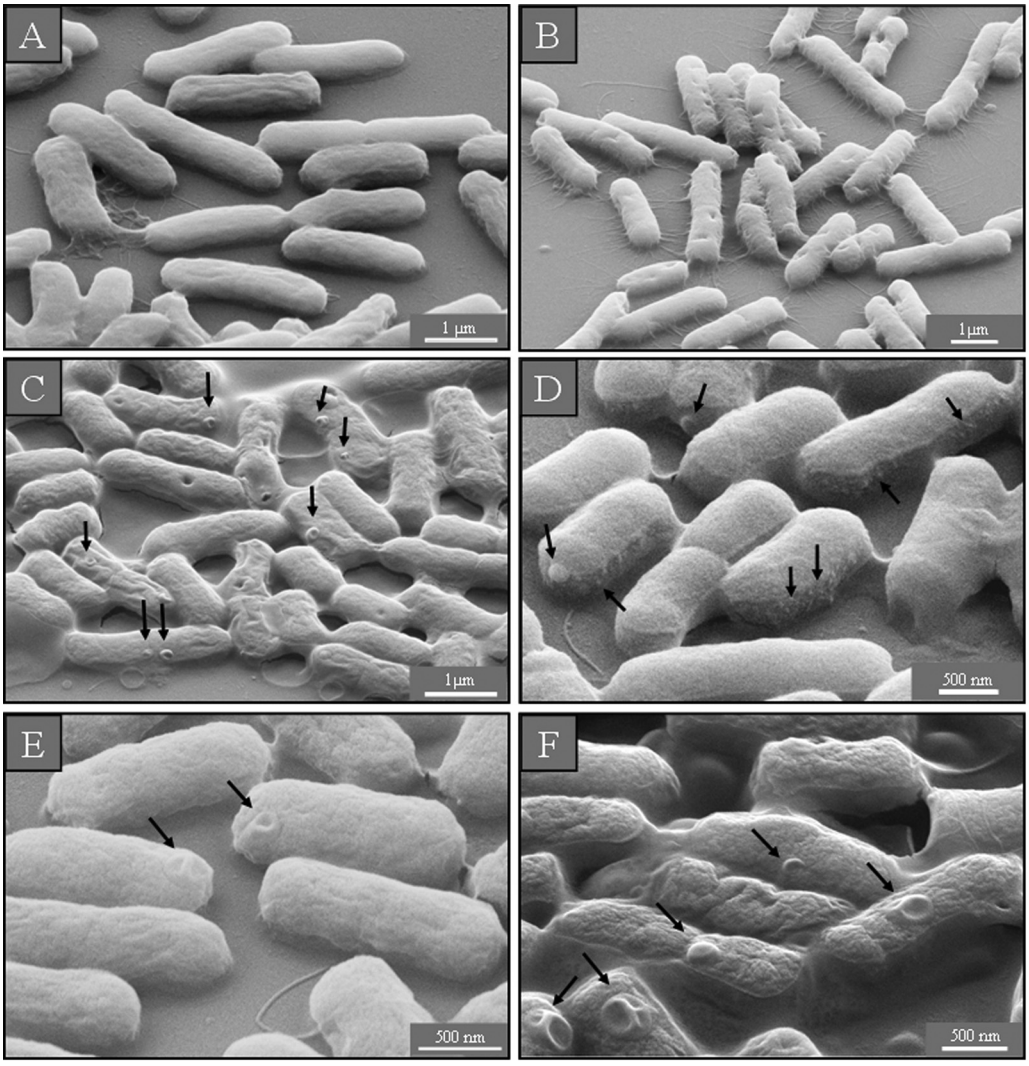

FIG. 2. SEM micrographs of untreated *E. coli* on silicon platelets. In isotonic medium the cells are long, intact, and evenly shaped (A), whereas in hypotonic medium their surface looks corrugated (B). After AMP treatment, the cells appear shorter and more compact (C to F). When incubated with a sub-MIC (C) or a supra-MIC (D) of GS and with a sub-MIC (E) or a supra-MIC (F) of PGLa, the cells show blisters on their surface, close to the polar and septal regions. When treated with a supra-MIC of GS, the bacteria additionally show small protruding bubbles on their surface (D).

both AMPs, however, the bacteria shortened to as little as 1 μm and significantly increased their compactness in both SEM preparations—on membrane filters and silicon platelets (Fig. 1C to F and 2C to F)—indicating that *E. coli* was not able to grow to maximum length. Along with the dimples on the surface of the control cells in low-salt medium, single blisters were observed after exposure to the sub-MIC of GS and both concentrations of PGLa (Fig. 2C, E, and F). Multiple blisters of various shapes on the cell surface were seen in the preparations on silicon after incubation with the supra-MIC of GS. The latter concentration induced the protrusion of numerous small bubbles of a few nanometers in size, which could be seen only in regions not covered with platinum (Fig. 2D).

In the control samples of *S. aureus* in LB medium with and without sodium chloride, the cells looked round and undamaged (Fig. 3A and B). After incubation with a sub-MIC of GS, some bacteria had holes in their cell wall (Fig. 3C), while a supra-MIC caused multiple dents (Fig. 3D) and lysed many cells (data not shown). After treatment of *S. aureus* with a sub-MIC of PGLa, we found some bacteria on the membrane filter preparations that had burst with deep craters in their cell wall (Fig. 3E), while at a supra-MIC numerous lysed cells and cell debris were observed (Fig. 3F).

Transmission electron microscopy. Untreated cells of *E. coli* in standard LB medium showed a normal cell shape with an undamaged structure of the inner membrane and an intact, slightly waved outer membrane. The periplasmic space was thin and had a uniform appearance (Fig. 4A). *E. coli* cells in medium with low ionic strength were characterized by an increased electron density of the cytosol. The periplasmic space of these cells looked hyperhydrated, but the inner and outer membranes remained intact (Fig. 4B). After incubation with a sub-MIC of GS, we observed the formation of additional membranous structures in the polar cell regions (Fig. 4C). At a

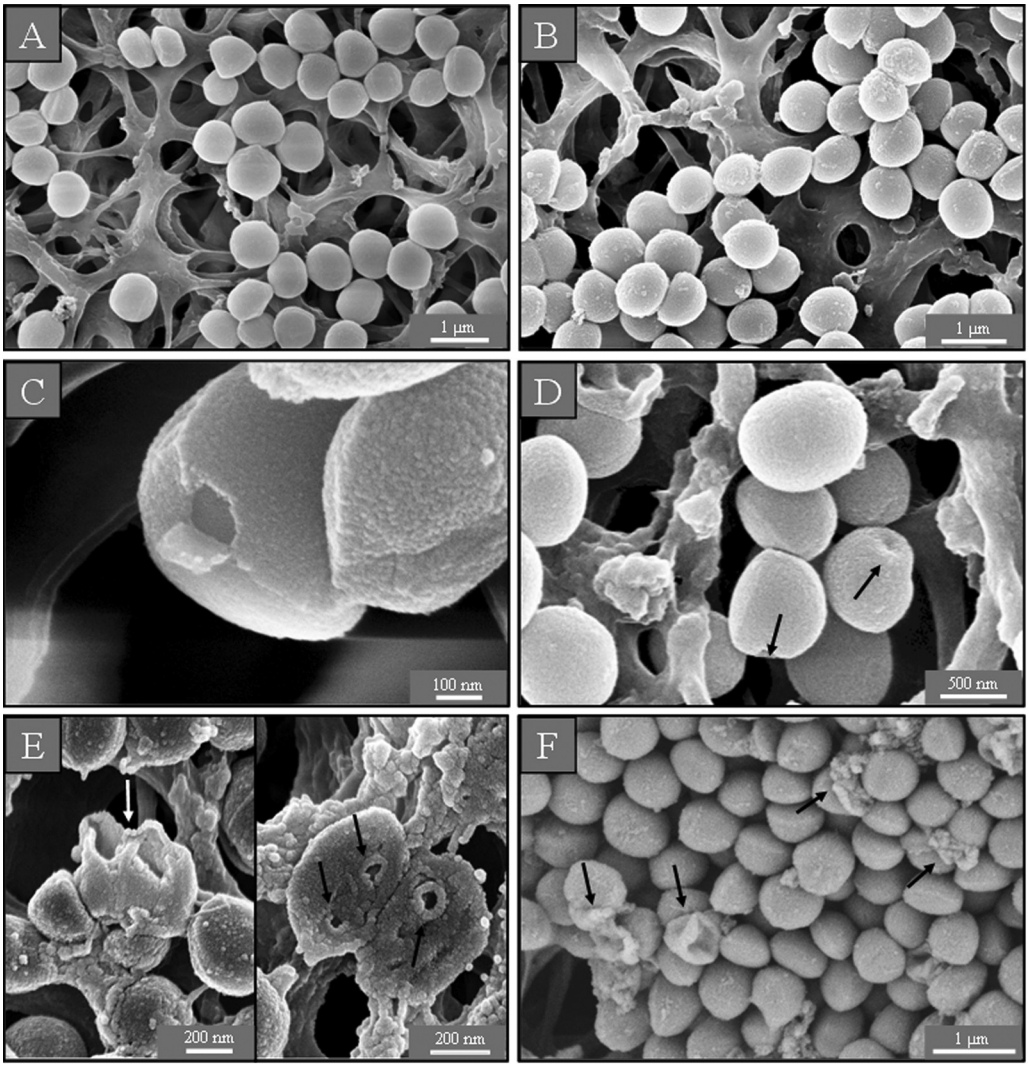

FIG. 3. SEM micrographs of untreated *S. aureus* on membrane filters. In isotonic (A) and hypotonic (B) medium, the cells are round and intact. After treatment with a sub-MIC of GS, some holes in the cells can be seen (C), while cells incubated with a supra-MIC of GS show dents (D). After treatment with a sub-MIC of PGLa, some deep craters and burst cells are observed (E), and after incubation with a supra-MIC of PGLa, some completely lysed cells are found (F).

supra-MIC, numerous bubbles were found to protrude from the outer cell membrane as noted also in the SEM sample, and the periplasmic space was completely filled with electron-dense material from the cytosol (Fig. 4D). No damage of either the inner or outer membranes was detected after treatment of *E. coli* with a sub-MIC of PGLa (data not shown). After incubation with a supra-MIC of PGLa, additional membranous structures were seen in the polar regions of *E. coli* (Fig. $4E_1$), and the periplasmic space had filled with electron-dense material (Fig. $4E_2$). In all cases the *E. coli* cells appeared turgid after AMP treatment, and no hyperhydration of the periplasm could be observed (Fig. 4C to E_2).

TEM micrographs of *S. aureus* in standard (Fig. 5A) and in salt-free (Fig. 5B) LB medium showed round, proliferating cells with intact cell walls and well-defined membranes. The intracellular DNA region displayed a heterogeneous electron density. After incubation with AMPs, however, the cytoplasm revealed a more uniform electron density. At a sub-MIC of GS, numerous spherical double-layered mesosome-like structures, as well as spherical non-membrane-enclosed bodies containing an electron density similar to that of the septal cell wall layer, could be observed in the cytoplasm (Fig. $5C_1$ and C_2). Mesosome-like structures could also be seen at a sub-MIC of PGLa (Fig. 5D). For a supra-MIC of GS no alterations except for the uniform electron density in the DNA region of *S. aureus* were detectable in comparison to the control (data not shown). At a supra-MIC of PGLa we observed many lysed cells (Fig. 5D).

DISCUSSION

Cationic amphiphilic antimicrobial peptides are electrostatically attracted by the negatively charged bacterial surface layers (32), and they get embedded into the hydrophobic regions of the lipid membranes, thereby causing membrane damage and disintegration. Accordingly, a three-step model has been suggested by atomic force microscopy (30), where first the

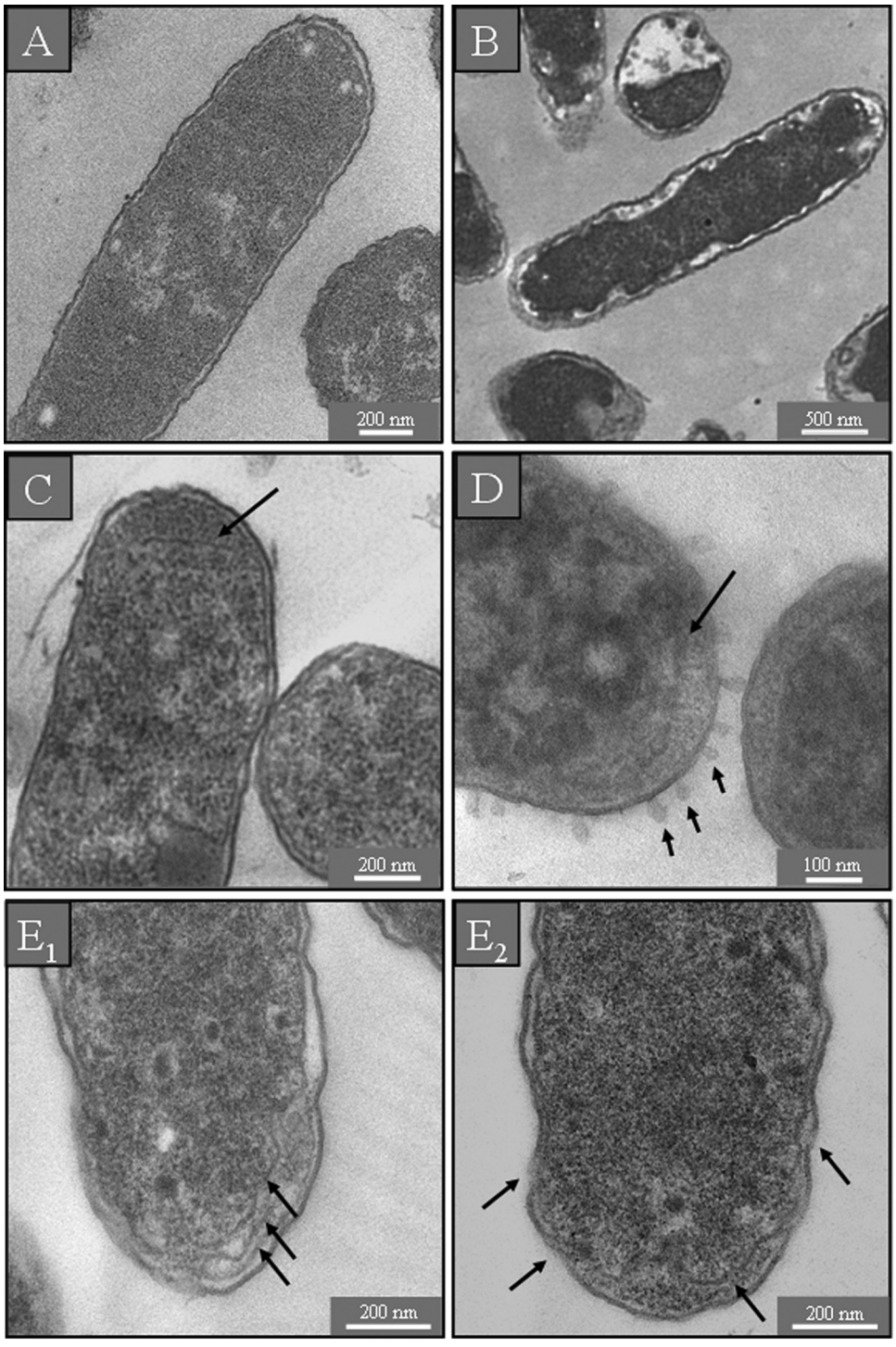

FIG. 4. TEM micrographs of untreated *E. coli*. In isotonic medium the inner and outer membranes are visible as continuous structures (A), and in hypotonic medium both membranes are still intact but the periplasmic space is swollen due to hyperhydration (B). After treatment with a sub-MIC of GS, some intracellular membrane stacks are formed near the polar regions of the cells (C), while a supra-MIC of GS causes the periplasmic space to be filled with electron-dense material and numerous bubbles protrude from the cell surface (D). After treatment with a supra-MIC of PGLa, the cells contain additional membranous structures (E_1), both membranes show interrupted stretches, and electron-dense material has accumulated in the periplasmic space (E_2). None of the bacteria treated with AMPs show any sign of hyperhydration (C to E_2).

outer membrane of Gram-negative bacteria is damaged, followed by permeabilization of the inner one and finally the total disintegration of both, causing leakage of the cytoplasmic contents. Our electron microscopy study has demonstrated that the impact of antimicrobial peptides on the bacterial cell passes through several stages, depending on the cell type, the peptide, and its concentration. After treatment of representative strains of the Gram-negative species *E. coli* (DSM 1103)

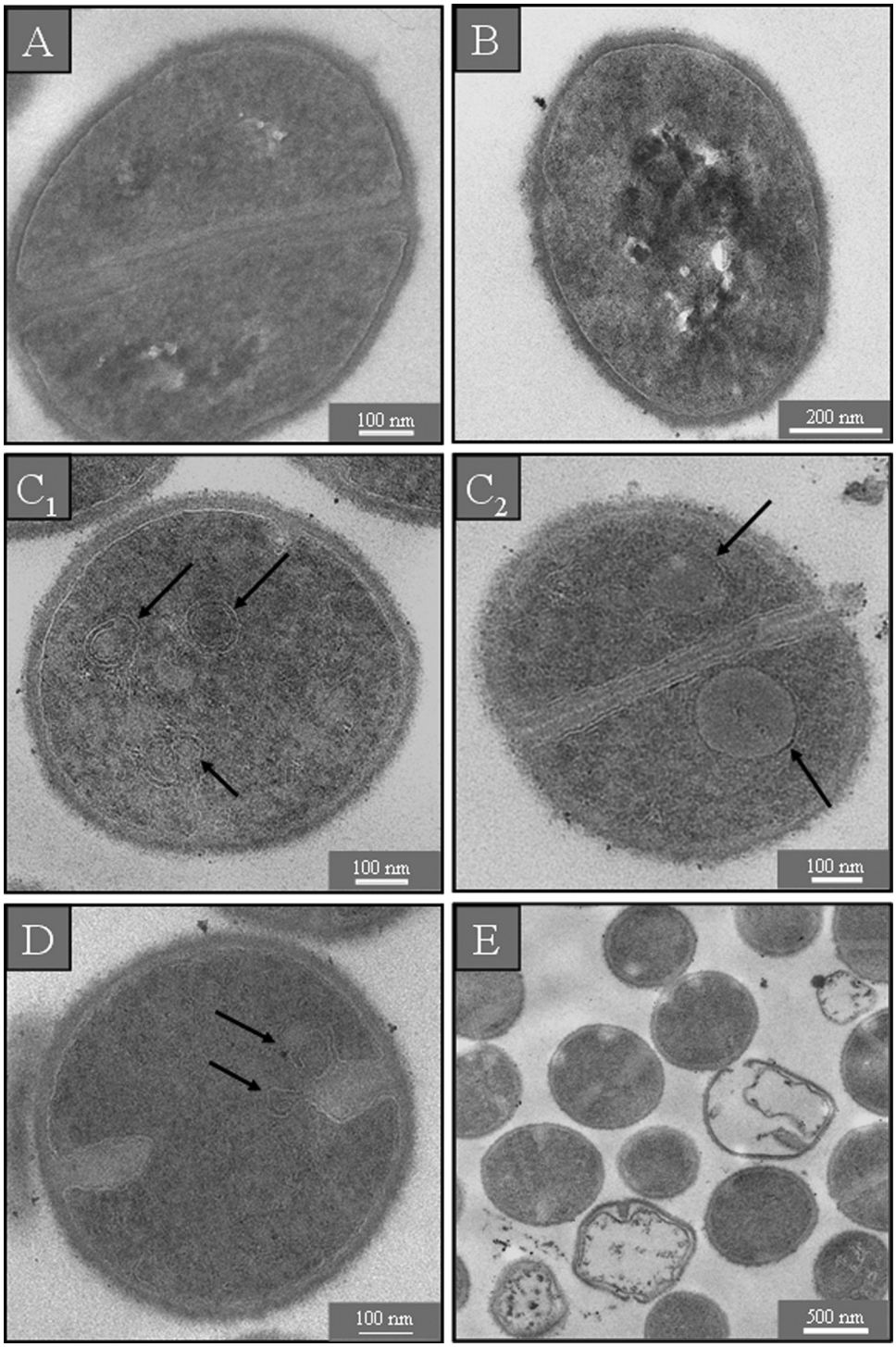

FIG. 5. TEM micrographs of untreated *S. aureus*. In isotonic (A) and hypotonic (B) medium, the cells are round and intact, with a well-defined cell membrane. The intracellular DNA region exhibits a highly inhomogeneous electron density. After treatment with a sub-MIC of GS (C_1) or PGLa (D), some mesosome-like structures are formed and non-membrane-enclosed bodies can be seen at a sub-MIC of GS (C_2). Incubation with a supra-MIC of PGLa shows some completely lysed cells (E).

and the Gram-positive species *S. aureus* (DSM 1104) with sub- and supra-MICs of PGLa or gramicidin S, several distinct signs of damage to the cell envelope were clearly observed in the SEM and TEM micrographs, such as blisters, protruding bubbles, membrane stacks, mesosomes, deep craters, and burst cells.

The appearance of blisters has been previously reported for the SMAP29 and PGYa peptides, which belong to the cathe-

licidin family (48, 51), and for isoforms of the HE2 peptide, which are similar to β-defensins (56). It was suggested that the positively charged AMPs can substitute for the Mg^{2+} ions in the lipopolysaccharide layer on the outer membrane of Gram-negative bacteria and thereby destabilize the outer surface (12). Such destabilization of the outer membrane would promote the penetration of AMPs and lead to a local disruption of the inner membrane, so that cytoplasmic material locally fills the periplasmic space. This causes the formation of blisters without disrupting the outer membrane. Our SEM images of *E. coli* incubated with a sub-MIC of GS or with sub- and supra-MICs of PGLa revealed such blisters on the cell surface, located mostly at the polar and septal regions (Fig. 2). This location may be explained by the preferential interaction of AMPs with negatively charged cardiolipin-rich domains, which have been visualized right at the polar and septal membrane regions of *E. coli* cells (38). Our TEM images of these cells treated with supra-MICs of both peptides—GS and PGLa—confirm the interaction of the peptides with the inner membrane, its disruption at the polar regions, and leakage of cytoplasm into the periplasmic space (Fig. 4D and E). The same topography of cell lesions at the polar ends and septal areas has been reported in an AFM study of *E. coli* with PGLa (35).

A critical alteration of the outer membrane was seen in our study only for a supra-MIC of GS, as the SEM images showed multiple small and a few large bubbles on the surface of *E. coli*, and TEM revealed numerous regularly distributed protrusions from the cell surface. AFM topography images of the *E. coli* strains 363 from the Pasteur Institute (12) and HB101 (35) treated with PGLa have been described in terms of a disintegration of the outer membrane into micelles and vesicle-like bodies, as well as larger cell lesions. In contrast, our EM observations support this possibility only for GS, not for PGLa. This differing observation suggests a higher efficiency of GS than of PGLa against *E. coli* DSM 1103 (Fig. 2D and 4D), and it indicates a difference in strain susceptibilities to various AMPs. However, a discrepancy in the terminology describing alterations of the cell surface by AFM and SEM (bubbles, micelles, and vesicle-like structures) is apparent, because neither method can determine whether these bubbles possess bilayer, monolayer, or disintegrated structures. Only via TEM did the ultrathin sections of *E. coli* cells treated with a supra-MIC of GS (Fig. 4D) allow us to determine that the protuberances had a continuous lamellar connection to the outer membrane.

Another significant impact of AMPs on *E. coli* was evident from the appearance of additional membrane structures in the polar regions at a sub-MIC of GS and a supra-MIC of PGLa (Fig. 4C and E). Given that the amphiphilic peptides get embedded in the lipid bilayer, a significant lateral expansion of the membrane area must occur upon binding and insertion of the AMPs (21). A concomitant membrane thinning, leading to further lateral expansion, has been described by micropipette aspiration, the single giant unilamellar vesicle (GUV) method, X-ray diffraction, and ^{31}P and ^{2}H solid-state NMR (33, 34, 52, 54). To accommodate this additional membrane area within the confined space of the cell wall, the formation of folded membrane stacks (in *E. coli*) and of mesosome structures (in *S. aureus*; see below) is a simple physicochemical consequence. It is important to note at this point that in a MIC assay the typical amount of AMPs needed to kill a bacterium is comparable to complete coverage of the cell surface (8, 36). Even though it is clear that not all these peptides will be bound to the inner membrane, the comparatively high number of molecules required for action will certainly have a significant impact on the lipid bilayer integrity and asymmetry (Shai-Matsuzaki-Huang model) (57) even under the sub-MIC conditions employed here.

Along the same lines, we can explain the adverse effect of even low AMP concentrations on the osmoregulatory capacity of the cells, which is evident from this TEM and SEM study. To avoid electrostatic screening by NaCl in LB medium, bacteria are commonly treated with AMPs in salt-free medium (28, 53). For comparison, we performed controls without AMPs in standard as well as in salt-free LB medium. These images showed no damage to the bacteria from the lack of salt but a distinct response to the osmotic gradient. Whereas the outer membrane of untreated *E. coli* in standard medium was slightly waved and the periplasmic space was uniformly distributed (Fig. 1A, 2A, and 4A), the control cells in salt-free medium possessed a hyperhydrated periplasm, an electron-dense cytosol, and several dents in the surface (Fig. 1B, 2B, and 4B). Even though the incubation with AMPs was done in salt-free medium, it is remarkable that the periplasmic space was not hyperhydrated, as the inner membrane was lying close to the outer membrane and all treated cells looked highly turgid (Fig. 4C to E). This appearance was even visible for a sub-MIC of PGLa in TEM, where we did not find any local cell lesions (data not shown) although the SEM images revealed several blisters (Fig. 2E). Moreover, a smoothing of the cell surface was demonstrated by SEM (Fig. 1 and 2) after incubation with either AMP, especially with a supra-MIC of GS, which confirms the highly turgid state of the cells seen in TEM. These observations clearly point to a breakdown of the osmoregulatory capacity of the bacteria.

In Fig. 6 we illustrate the impact of the AMPs on the osmoregulation of the cells, when they are exposed to low-salt medium such that water will flow into the cytosol (Fig. 6B). When the cells start to swell, mechanosensitive channels in the inner membrane will open and release water, solutes, and ions into the periplasm, to avoid bursting (39, 40). It is known that *E. coli* and other Gram-negative bacteria respond to osmotic downshock by increasing the production of negatively charged membrane-derived oligosaccharides (MDO) and accumulating them in the periplasmic space (24) (Fig. 6C). The MDO molecules thus reduce the osmotic pressure difference across the inner membrane and can act as a kind of hydrogel, which binds the cations and water. Cells in salt-free medium therefore show a dark cytoplasm and a wide periplasmic space, similar to plasmolysis in hypertonic media (25, 37) (Fig. 4B). In our AMP-treated cells, however, the osmoregulation is evidently repressed, because the cells looked turgid and the periplasmic space was very thin (Fig. 1C to F, 2C to F, 4C to E, and 6D). This suggests that the AMPs are able to short-circuit the osmoregulatory response of *E. coli*, by rendering the inner membrane leaky. Again, this effect can be simply attributed to the insertion of the amphiphilic peptides into the lipid bilayer, which induces local defects in lipid packing and causes enhanced permeability even at a low AMP concentration. As a result of the increased influx of water into the cytoplasm, the

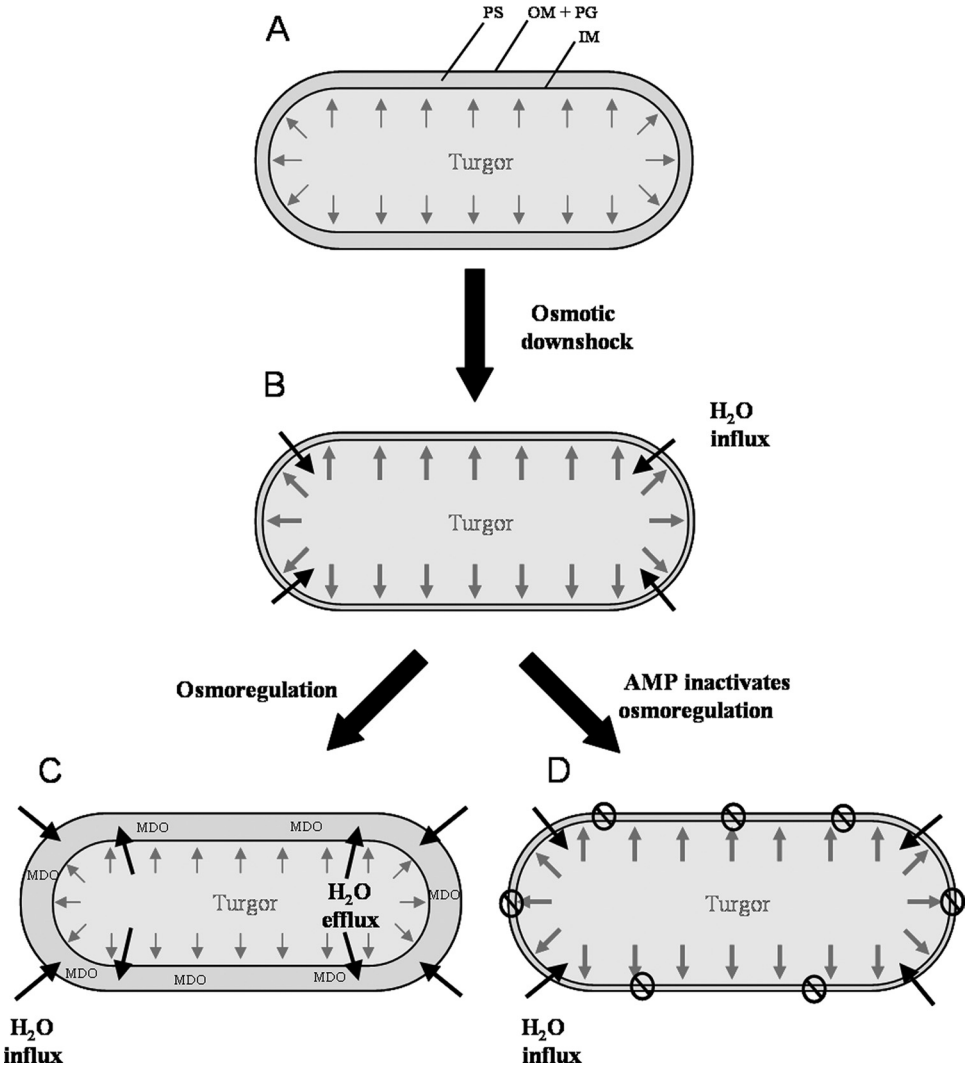

FIG. 6. Illustration of the cellular response to osmotic downshock in the absence and presence of AMPs. (A) Cell in isosmotic medium; (B) cell shortly after osmotic downshock; (C) healthy cellular response to water influx; (D) cell incapable of osmoregulation after AMP treatment, which renders the inner membrane inherently leaky due to peptide binding. IM, inner membrane; OM, outer membrane; PG, peptidoglycan; PS, periplasmic space; MDO, membrane-derived oligosaccharides.

turgor pressure increases and the cell is no longer able to compensate for it. This interpretation is in full agreement with the observed dissociation between the initial membrane perturbation and the ultimate cell death (19, 55). For instance, *Pseudomonas aeruginosa* is relatively resistant to GS, but a rapid depolarization of the cytoplasmic membrane has been observed by the reduction in di-SC35 fluorescence even at low concentrations where no killing occurs (58). Eventually, at a high peptide concentration a rupture of the cytoplasmic membrane leads to leakage of cytoplasmic material into the periplasmic space, as seen in our images described above. Both the inner membrane leakage and the outer membranous protuberances around the cells at a supra-MIC of GS are evidence of an extreme turgor pressure.

On the basis of our results, we propose the following multistage model for the interaction of AMPs, such as GS and PGLa, with the cell surface of Gram-negative bacteria: (i) the outer membrane is destabilized and penetrated; (ii) the peptides bind to cardiolipin-rich domains in the polar and septal regions of the inner membrane; and (iii) (*a*) a low AMP concentration (a sub-MIC) merely induces leakage of the inner membrane, which under low-salt conditions interferes with the osmoregulation of the cells; *(b)* higher peptide concentrations lead to local disruption of the inner membrane and the release of cell content into the periplasmic space, which causes the formation of blisters; and *(c)* an even higher concentration (a supra-MIC) results in a disintegration of the outer membrane and complete cell lysis.

Also in the case of the Gram-positive *S. aureus* cells, TEM showed differences in the control samples and AMP-treated bacteria. While the control cells displayed a DNA region with high contrast in electron density, the cytoplasm of treated cells had a homogeneous appearance. This observation suggests an influence of both peptides on DNA replication and transcription. Indeed, an upregulation of important cell activities has been previously observed in AMP-treated *S. aureus* by tran-

scriptional analysis, with regard to efflux pumping, aerobic energy generation, and cell wall and lipid biosynthesis (42). Our TEM images clearly show an interaction of the peptides with the lipid bilayer of *S. aureus*, attributed to peptide insertion and lateral expansion of the membrane area. We observed a bloating and spreading of the cytoplasmic membrane already at a sub-MIC of GS and PGLa (Fig. $5C_2$ and D). The budding of spherical mesosomes as intracellular bilayered membranes was revealed at sub-MICs of GS and PGLa (Fig. $5C_1$ and D), like those shown by Shimoda et al. (47) after incubation with defensin. Additionally, some large non-membrane-enclosed bodies with an electron density similar to that of the septal murein layer were seen in *S. aureus* cells at a sub-MIC of GS (Fig. $5C_2$). In coccoid cells like those of *S. aureus*, it is known that new peptidoglycan is inserted only at the division septum (44). We may thus speculate that exposure to sub-MICs of GS leads to an accumulation of peptidoglycan and teichoic acid precursors, which are synthesized in such bodies in the cytoplasm under conditions where the translocation of lipid-linked precursors from the cytoplasmic side to the outer side of the membrane is disturbed. Furthermore, several dents, holes, and craters were seen on the surface of bacteria incubated with GS or PGLa when they were prepared on a filter paper and observed with SEM, indicative of a mechanical rupture of the membrane and cell wall.

Conclusions. This study demonstrates that both SEM and TEM are needed as complementary techniques to gain insight into AMP action, by revealing not only cell surface effects but also intracellular alterations. Furthermore, certain details of the sample preparation procedure can influence the visualization results. Here we describe for the first time a new protocol for depositing bacteria on silicon platelets by means of direct fixation, without a dehydration step, which allowed us to detect blisters in the polar and septal regions of *E. coli*. On the other hand, preparations of *S. aureus* on a membrane filter worked best to reveal holes and deep craters on the surface of lysed cells, as the bacteria were first brought onto the support before fixation and dehydration.

Comprehensive EM analysis allowed us to visualize the idea that AMPs cause multiple stresses on the membranes of *E. coli*. Even at low concentrations, GS and PGLa can permeabilize and penetrate the outer membrane by replacing divalent cations. Insertion of the peptides into the inner membrane leads to a lateral expansion of the lipid bilayer, which becomes folded into membranous stacks near the polar regions of the cell. At the same time, peptide binding destabilizes the inner membrane and makes it leaky, so that in medium with low ionic strength the cells lose their capability to regulate the turgor pressure. Remarkably, only a supra-MIC of GS caused a visible disintegration of the outer membrane leading to the appearance of regular protruding bubbles. In the case of *S. aureus*, intracellular membrane-enclosed mesosome structures are formed, presumably also to compensate for the area increase of the cell membrane upon peptide binding.

ACKNOWLEDGMENTS

We thank N. S. Churilova (IEGM of Russia Academy of Science, Perm, Russia) for helpful recommendations concerning TEM sample preparation and critical discussion of the results and P. Wadhwani for the PGLa synthesis. We are grateful to Sergii Afonin for kindly helping with the manuscript.

The DFG Center for Functional Nanostructures is acknowledged (TP E1.2 and Z) for financial support.

REFERENCES

1. **Afonin, S., U. H. N. Dürr, P. Wadhwani, J. B. Salgado, and A. S. Ulrich.** 2008. Solid state NMR structure analysis of the antimicrobial peptide gramicidin S in lipid membranes: concentration-dependent re-alignment and self-assembly as a β-barrel. Top. Curr. Chem. **273:**139–154.
2. **Afonin, S., R. W. Glaser, M. Berditchevskaia, P. Wadhwani, K. H. Guhrs, U. Mollmann, A. Perner, and A. S. Ulrich.** 2003. 4-Fluorophenylglycine as a label for 19F NMR structure analysis of membrane-associated peptides. Chembiochem **4:**1151–1163.
3. **Afonin, S., S. L. Grage, M. Ieronimo, P. Wadhwani, and A. S. Ulrich.** 2008. Temperature-dependent transmembrane insertion of the amphiphilic peptide PGLa in lipid bilayers observed by solid state (19)F NMR spectroscopy. J. Am. Chem. Soc. **130:**16512–16514.
4. **Amsterdam, D.** 1996. Susceptibility testing of antimicrobials in liquid media, p. 52–111. *In* V. Lorian (ed.), Antibiotics in laboratory medicine, 4th ed. Williams & Wilkins, Baltimore, MD.
5. **Anderson, R. C., R. G. Haverkamp, and P. L. Yu.** 2004. Investigation of morphological changes to *Staphylococcus aureus* induced by ovine-derived antimicrobial peptides using TEM and AFM. FEMS Microbiol. Lett. **240:** 105–110.
6. **Bechinger, B., M. Zasloff, and S. J. Opella.** 1998. Structure and dynamics of the antibiotic peptide PGLa in membranes by solution and solid-state nuclear magnetic resonance spectroscopy. Biophys. J. **74:**981–987.
7. **Berditsch, M., S. Afonin, and A. S. Ulrich.** 2007. The ability of *Aneurinibacillus migulanus* (*Bacillus brevis*) to produce the antibiotic gramicidin S is correlated with phenotype variation. Appl. Environ. Microbiol. **73:**6620–6628.
8. **Blazyk, J., R. Wiegand, J. Klein, J. Hammer, R. M. Epand, R. F. Epand, W. L. Maloy, and U. P. Kari.** 2001. A novel linear amphipathic beta-sheet cationic antimicrobial peptide with enhanced selectivity for bacterial lipids. J. Biol. Chem. **276:**27899–27906.
9. **Bourinbaiar, A. S., and C. F. Coleman.** 1997. The effect of gramicidin, a topical contraceptive and antimicrobial agent with anti-HIV activity, against herpes simplex viruses type 1 and 2 in vitro. Arch. Virol. **142:**2225–2235.
10. **Chinchar, V. G., L. Bryan, U. Silphadaung, E. Noga, D. Wade, and L. Rollins-Smith.** 2004. Inactivation of viruses infecting ectothermic animals by amphibian and piscine antimicrobial peptides. Virology **323:**268–275.
11. **Cruciani, R. A., J. L. Barker, S. R. Durell, G. Raghunathan, H. R. Guy, M. Zasloff, and E. F. Stanley.** 1992. Magainin 2, a natural antibiotic from frog skin, forms ion channels in lipid bilayer membranes. Eur. J. Pharmacol. **226:**287–296.
12. **da Silva, A., Jr., and O. Teschke.** 2003. Effects of the antimicrobial peptide PGLa on live *Escherichia coli*. Biochim. Biophys. Acta **1643:**95–103.
13. **Duclohier, H.** 1994. Anion pores from magainins and related defensive peptides. Toxicology **87:**175–188.
14. **Friedrich, C. L., D. Moyles, T. J. Beveridge, and R. E. Hancock.** 2000. Antibacterial action of structurally diverse cationic peptides on gram-positive bacteria. Antimicrob. Agents Chemother. **44:**2086–2092.
15. **Gause, G. F., and M. G. Brazhnikova.** 1944. Gramicidin S and its use in the treatment of infected wounds. Nature **154:**703.
16. **Gause, G. F., and M. G. Brazhnikova.** 1944. Gramicidin S. Origin and mode of action. Lancet **247:**715–716.
17. **Glaser, R. W., C. Sachse, U. H. Durr, P. Wadhwani, and A. S. Ulrich.** 2004. Orientation of the antimicrobial peptide PGLa in lipid membranes determined from 19F-NMR dipolar couplings of 4-CF3-phenylglycine labels. J. Magn. Reson. **168:**153–163.
18. **Grotenbreg, G. M., M. S. Timmer, A. L. Llamas-Saiz, M. Verdoes, G. A. van der Marel, M. J. van Raaij, H. S. Overkleeft, and M. Overhand.** 2004. An unusual reverse turn structure adopted by a furanoid sugar amino acid incorporated in gramicidin S. J. Am. Chem. Soc. **126:**3444–3446.
19. **Gunaratna, K. R., M. Anderson, and L. Good.** 2002. Microbial membrane-permeating peptides and their applications, p. 377–396. *In* U. Langel (ed.), Cell-penetrating peptides: process and applications. CRC Press LLC, Boca Raton, FL.
20. **Hancock, R. E.** 1997. Peptide antibiotics. Lancet **349:**418–422.
21. **Huang, H. W.** 2009. Free energies of molecular bound states in lipid bilayers: lethal concentrations of antimicrobial peptides. Biophys. J. **96:**3263–3272.
22. **Huang, H. W., F. Y. Chen, and M. T. Lee.** 2004. Molecular mechanism of peptide-induced pores in membranes. Phys. Rev. Lett. **92:**198304.
23. **Jelokhani-Niaraki, M., L. H. Kondejewski, S. W. Farmer, R. E. Hancock, C. M. Kay, and R. S. Hodges.** 2000. Diastereoisomeric analogues of gramicidin S: structure, biological activity and interaction with lipid bilayers. Biochem. J. **349:**747–755.
24. **Kennedy, E. P.** 1982. Osmotic regulation and the biosynthesis of membrane-derived oligosaccharides in *Escherichia coli*. Proc. Natl. Acad. Sci. U. S. A. **79:**1092–1095.

25. **Koch, A. L.** 1998. The biophysics of the gram-negative periplasmic space. Crit. Rev. Microbiol. **24:**23–59.
26. **Kondejewski, L. H., S. W. Farmer, D. S. Wishart, R. E. Hancock, and R. S. Hodges.** 1996. Gramicidin S is active against both gram-positive and gram-negative bacteria. Int. J. Pept. Protein Res. **47:**460–466.
27. **Kondejewski, L. H., S. W. Farmer, D. S. Wishart, C. M. Kay, R. E. Hancock, and R. S. Hodges.** 1996. Modulation of structure and antibacterial and hemolytic activity by ring size in cyclic gramicidin S analogs. J. Biol. Chem. **271:**25261–25268.
28. **Kondejewski, L. H., M. Jelokhani-Niaraki, S. W. Farmer, B. Lix, C. M. Kay, B. D. Sykes, R. E. Hancock, and R. S. Hodges.** 1999. Dissociation of antimicrobial and hemolytic activities in cyclic peptide diastereomers by systematic alterations in amphipathicity. J. Biol. Chem. **274:**13181–13192.
29. **Lehrer, R. I., A. Barton, K. A. Daher, S. S. Harwig, T. Ganz, and M. E. Selsted.** 1989. Interaction of human defensins with *Escherichia coli*. Mechanism of bactericidal activity. J. Clin. Invest. **84:**553–561.
30. **Li, A., P. Y. Lee, B. Ho, J. L. Ding, and C. T. Lim.** 2007. Atomic force microscopy study of the antimicrobial action of Sushi peptides on Gram negative bacteria. Biochim. Biophys. Acta **1768:**411–418.
31. **Llamas-Saiz, A. L., G. M. Grotenbreg, M. Overhand, and M. J. van Raaij.** 2007. Double-stranded helical twisted beta-sheet channels in crystals of gramicidin S grown in the presence of trifluoroacetic and hydrochloric acids. Acta Crystallogr. D Biol. Crystallogr. **63:**401–407.
32. **Lohner, K., and F. Prossnigg.** 2009. Biological activity and structural aspects of PGLa interaction with membrane mimetic systems. Biochim. Biophys. Acta **1788:**1656–1666.
33. **Longo, M. L., A. J. Waring, L. M. Gordon, and D. A. Hammer.** 1998. Area expansion and permeation of phospholipid membrane bilayers by influenza fusion peptides and melittin. Langmuir **14:**2385–2395.
34. **Ludtke, S., K. He, and H. Huang.** 1995. Membrane thinning caused by magainin 2. Biochemistry **34:**16764–16769.
35. **Meincken, M., D. L. Holroyd, and M. Rautenbach.** 2005. Atomic force microscopy study of the effect of antimicrobial peptides on the cell envelope of *Escherichia coli*. Antimicrob. Agents Chemother. **49:**4085–4092.
36. **Melo, M. N., R. Ferre, and M. A. Castanho.** 2009. Antimicrobial peptides: linking partition, activity and high membrane-bound concentrations. Nat. Rev. Microbiol. **7:**245–250.
37. **Meury, J., and G. Devilliers.** 1999. Impairment of cell division in tolA mutants of *Escherichia coli* at low and high medium osmolarities. Biol. Cell **91:**67–75.
38. **Mileykovskaya, E., and W. Dowhan.** 2000. Visualization of phospholipid domains in *Escherichia coli* by using the cardiolipin-specific fluorescent dye 10-N-nonyl acridine orange. J. Bacteriol. **182:**1172–1175.
39. **Miller, K. J., E. P. Kennedy, and V. N. Reinhold.** 1986. Osmotic adaptation by gram-negative bacteria: possible role for periplasmic oligosaccharides. Science **231:**48–51.
40. **Morbach, S., and R. Kramer.** 2002. Body shaping under water stress: osmosensing and osmoregulation of solute transport in bacteria. Chembiochem **3:**384–397.
41. **Nir-Paz, R., M. C. Prevost, P. Nicolas, A. Blanchard, and H. Wroblewski.** 2002. Susceptibilities of *Mycoplasma fermentans* and *Mycoplasma hyorhinis* to membrane-active peptides and enrofloxacin in human tissue cell cultures. Antimicrob. Agents Chemother. **46:**1218–1225.
42. **Pag, U., M. Oedenkoven, V. Sass, Y. Shai, O. Shamova, N. Antcheva, A. Tossi, and H. G. Sahl.** 2008. Analysis of in vitro activities and modes of action of synthetic antimicrobial peptides derived from an alpha-helical 'sequence template.' J. Antimicrob. Chemother. **61:**341–352.
43. **Reimer, L. (ed.).** 1995. Series in optical sciences, vol. 71. Energy-filtering transmission electron microscopy, p. 347–400. Springer-Verlag, New York, NY.
44. **Reusch, V. M., Jr., and M. M. Burger.** 1973. The bacterial mesosome. Biochim. Biophys. Acta **300:**79–104.
45. **Ruden, S., K. Hilpert, M. Berditsch, P. Wadhwani, and A. S. Ulrich.** 2009. Synergistic interaction between silver nanoparticles and membrane-permeabilizing antimicrobial peptides. Antimicrob. Agents Chemother. **53:**3538–3540.
46. **Shai, Y.** 1999. Mechanism of the binding, insertion and destabilization of phospholipid bilayer membranes by alpha-helical antimicrobial and cell nonselective membrane-lytic peptides. Biochim. Biophys. Acta **1462:**55–70.
47. **Shimoda, M., K. Ohki, Y. Shimamoto, and O. Kohashi.** 1995. Morphology of defensin-treated *Staphylococcus aureus*. Infect. Immun. **63:**2886–2891.
48. **Skerlavaj, B., M. Benincasa, A. Risso, M. Zanetti, and R. Gennaro.** 1999. SMAP-29: a potent antibacterial and antifungal peptide from sheep leukocytes. FEBS Lett. **463:**58–62.
49. **Soravia, E., G. Martini, and M. Zasloff.** 1988. Antimicrobial properties of peptides from *Xenopus* granular gland secretions. FEBS Lett. **228:**337–340.
50. **Tennessen, J. A.** 2005. Molecular evolution of animal antimicrobial peptides: widespread moderate positive selection. J. Evol. Biol. **18:**1387–1394.
51. **Tiozzo, E., G. Rocco, A. Tossi, and D. Romeo.** 1998. Wide-spectrum antibiotic activity of synthetic, amphipathic peptides. Biochem. Biophys. Res. Commun. **249:**202–206.
52. **Wi, S., and C. Kim.** 2008. Pore structure, thinning effect, and lateral diffusive dynamics of oriented lipid membranes interacting with antimicrobial peptide protegrin-1: 31P and 2H solid-state NMR study. J. Phys. Chem. B **112:** 11402–11414.
53. **Wu, M., and R. E. Hancock.** 1999. Interaction of the cyclic antimicrobial cationic peptide bactenecin with the outer and cytoplasmic membrane. J. Biol. Chem. **274:**29–35.
54. **Yamashita, Y., S. M. Masum, T. Tanaka, and M. Yamazaki.** 2002. Shape changes of giant unilamellar vesicles of phosphatidylcholine induced by a de novo designed peptide interacting with their membrane interface. Langmuir **18:**9638–9641.
55. **Yeaman, M. R., and N. Y. Yount.** 2003. Mechanisms of antimicrobial peptide action and resistance. Pharmacol. Rev. **55:**27–55.
56. **Yenugu, S., K. G. Hamil, F. S. French, and S. H. Hall.** 2004. Antimicrobial actions of the human epididymis 2 (HE2) protein isoforms, HE2alpha, HE2beta1 and HE2beta2. Reprod. Biol. Endocrinol. **2:**61.
57. **Zasloff, M.** 2002. Antimicrobial peptides of multicellular organisms. Nature **415:**389–395.
58. **Zhang, L., P. Dhillon, H. Yan, S. Farmer, and R. E. Hancock.** 2000. Interactions of bacterial cationic peptide antibiotics with outer and cytoplasmic membranes of *Pseudomonas aeruginosa*. Antimicrob. Agents Chemother. **44:**3317–3321.